Int J Adv Manuf Technol (2012) 60:977–984
DOI 10.1007/s00170-011-3682-y

ORIGINAL ARTICLE

Micro electrochemical milling of complex structures by using in situ fabricated cylindrical electrode

Yong Liu · Di Zhu · Linsen Zhu

Received: 1 April 2011 / Accepted: 3 October 2011 / Published online: 18 October 2011

Abstract A micro electrochemical milling by layer process is presented in this paper. Because of no tool wear in electrochemical micromachining, a very thin tungsten electrode is used as the tool cathode. By applying ultrashort pulses, dissolution of a workpiece can be restricted to the region very close to the electrode. First, the mathematical model of micro electrochemical milling by layer is established to ensure a good shape precision. Second, the micrometer scale cylindrical electrode is fabricated in situ by electrochemical etching for the production of micro structures. And then, effects of machining parameters on the side gap variation in electrochemical milling process have been studied experimentally. Finally, some 2D micro shapes and 3D complex micro structures with physical dimension of several 10 μm have been obtained.

Keywords Electrochemical · Micromachining · Milling by layer · Micro shapes · Complex structures

1 Introduction

With the development of Micro-Electro-Mechanical System (MEMS), micromachining techniques have become a hot issue in modern industry. Micro-scale metal complex structures have a wide range of application in many fields, including biomedicine and aviation. For example, there are many micro metal parts or components in the impeller unit, transmission unit, and manipulation unit of micro air vehicle. As so far, micromachining techniques [1] include: lithography, electro discharge machining (EDM), ultrasonic machining, electrochemical machining, and so on. Compared to EDM, electrochemical machining is an electrochemical dissolution process that has many advantages, such as no tool wear, stress-free, and smooth surfaces, and also has the ability to machine complex structures in materials, regardless of their hardness and high strength, high tension, or whether they are heat-resistant materials.

Many research attempts on electrochemical micromachining (EMM) have been done. Recent researches focus on EMM with the ultrahigh-frequency pulse current. It has been reported that material removal is strongly localized when ultrahigh-frequency pulse current is used instead of conventional DC or low-frequency pulse current [2–5].

Micro electrochemical milling can be applied to the fabrication of micro metal parts [6]. However, the micron scale electrode is breakable in the clamping process. To solve the problem, in situ fabricated cylindrical electrode is proposed in this paper. The micro cylindrical electrode with the diameter of 10 μm has been in situ fabricated. The mechanism and mathematical model of the machining process are studied. Some typical 2D and 3D micro metal structures have been obtained on the hard-to-cut material–super alloy plate.

2 Principle of EMM

Figure 1 illustrates the principle of the micro electrochemical milling. In the machining process, pulse voltage is

Y. Liu (✉) · L. Zhu
Associated Engineering Research Center of Mechanics and Mechatronic Equipment, Shandong University,
Weihai 264209, China
e-mail: rzliuyong@163.com

D. Zhu
College of Mechanical and Electrical Engineering,
Nanjing University of Aeronautics and Astronautics,
Nanjing 210016, China

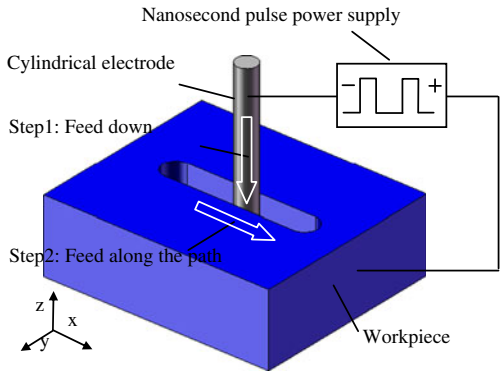

Fig. 1 Schematic diagram of micro electrochemical milling

applied between workpiece and cylindrical electrode in an electrolyte cell. Workpiece is electrochemically removed, and narrow groove is produced as the cathode feeds along the scheduled path. The machining process is divided into two steps. Step 1: the electrode feeds down to an appointed depth as the starting point. Step 2: the electrode feeds along the scheduled path in the X–Y plane to accomplish a layer of processing, and steps 1 and 2 are interchanged until the machining is finished.

Step 1 Feeding down

Step 1 is a drilling hole process in effect. The machining accuracy of the proposed method mainly depends on the side gap $\triangle s_x$. The key problem of improving the machining accuracy is how to minimize the hole entrance diameter. Figure 2 illustrates the side gap in the drilling process.

In Fig. 2, $\triangle b_z$ is the inter-electrode frontal gap, $\triangle s_x$ is the side gap, the feed rate of electrode is v_{cz}, and the dissolution rate of material in position A is:

$$V_A = \frac{dx}{dt} = \frac{\omega\sigma(\Phi - \delta E)}{x} \tag{1}$$

That is:

$$\int x dx = \int \omega\sigma(\Phi - \delta E)\, dt \tag{2}$$

where ω is electrochemical equivalence of anode metal, σ is electrolyte conductivity, Φ is machining voltage, and δE is the sum of electrode potentials.

$x = x_0$ at $t = 0$, solving the integral of (2) gives:

$$x = \sqrt{2\omega\sigma(\Phi - \delta E)t + {x_0}^2} \tag{3}$$

The inter-electrode frontal gap $\triangle b_z$ is given by:

$$\Delta b_z = \frac{\omega\sigma(\Phi - \delta E)}{v_{cz}} \tag{4}$$

When the diameter of the electrode is in micron scale, $x_0 \approx \triangle b_z$ and $\triangle s_x = x$ at:

$$t = \frac{L}{V_{cz}} \tag{5}$$

where L is the milling layer thickness. From (3) to (5), $\triangle s_x$ can be given approximatively:

$$\Delta s_x = \sqrt{2\omega\sigma(\Phi - \delta E)t + {\Delta b_z}^2} \tag{6}$$
$$= \sqrt{\frac{2\omega\sigma(\Phi - \delta E)L}{v_{cz}} + \left[\frac{\omega\sigma(\Phi - \delta E)}{v_{cz}}\right]^2}$$

So the hole entrance diameter is determined by:

$$D = d + 2\,\Delta s_x \tag{7}$$

where d is electrode diameter. So, the hole entrance diameter is affected by lots of factors, such as electrode diameter d, milling layer thickness L, the feed rate v_{cz}, the applied voltage Φ, the electrolyte conductivity σ, and so on.

Step 2 Feeding along the path

When the electrode feeds along the scheduled path in plane X–Y, the machining localization of the proposed method mainly depends on the side gap $\triangle s_y$. The key problem of improving the machining localization is how to minimize the groove width. Figure 3 illustrates the side gap in plane milling process.

According to the same derivation method as $\triangle s_y$ in step 1, the side gap $\triangle s_y$ can be obtained as the following expression:

$$\Delta s_y = \sqrt{2d\,\Delta b_x + {\Delta b_x}^2} \tag{8}$$
$$= \sqrt{2d\frac{\omega\sigma(\Phi - \delta E)}{v_{cx}} + \left[\frac{\omega\sigma(\Phi - \delta E)}{v_{cx}}\right]^2}$$

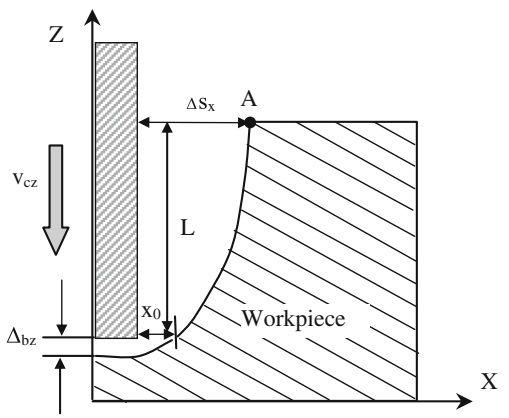

Fig. 2 Sketch of feeding down

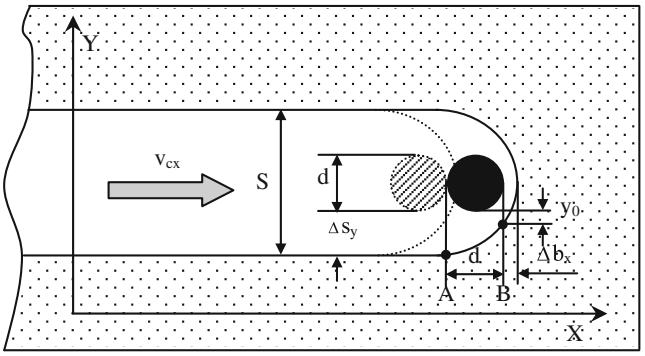

Fig. 3 Sketch of feeding along the X–Y plane

where Δb_x is the inter-electrode frontal gap, and v_{cx} is the feed rate of electrode.

So the groove width S is determined by:

$$S = d + 2\,\Delta s_y \tag{9}$$

In order to ensure a good shape precision, the hole entrance diameter D in step 1 and the groove width S in step 2 should have the following relationships:

$$D \le S \Rightarrow\ \Delta s_x \le\ \Delta s_y \tag{10}$$

That is:

$$\frac{2\omega\sigma(\Phi - \delta\mathrm{E})L}{v_{cz}} + \left[\frac{\omega\sigma(\Phi - \delta\mathrm{E})}{v_{cz}}\right]^2 \le 2d\frac{\omega\sigma(\Phi - \delta\mathrm{E})}{v_{cx}} + \left[\frac{\omega\sigma(\Phi - \delta\mathrm{E})}{v_{cx}}\right]^2 \tag{11}$$

When the feed rate v_{cz} in step 1 equals the feed rate v_{cx} in step 2, the expression above can be simplified as follows:

$$L \le d \tag{12}$$

So, a conclusion can be reached: in order to ensure a good shape precision, the milling layer thickness L cannot be great than the cylindrical electrode diameter d which is used in the machining process.

Equations (6) and (8) show that the diameter of the electrode is decisive for the reduction of both the groove width and the hole entrance diameter. Therefore, in situ fabrication of cylindrical electrode is proposed in this study to fabricate micrometer scale electrode. And for achieving a good machining quality, sets of experiments have been carried out in the following experimental section.

3 Experimental system and measuring instrument

The developed electrochemical micro milling setup as shown in Fig. 4 consists of various subcomponents, including electrodes unit, electrolyte flow system, servo-control feed unit, data acquisition system, etc. The micron scale cylindrical tungsten pin which is fabricated by electrochemical etching is used as cathode tool. The high-frequency pulse voltage was applied to the electrodes. H_2SO_4, 0.2 M, was preferred because the acid electrolyte usually produces much less by-product than common salt electrolytes, which is important for a steady machining process in a so small machining gap.

The stability is most important for this micro machining with the gap of several micrometers. If the tool feed rate is too high, the tool will come in contact with the workpiece and cause short circuit. So, a safety system is necessarily built in the EMM setup. When a short circuit is detected, the servo motor will stop and move backward along the path of feed forward immediately until the danger is clear.

The motion control system consisted of a precise XYZ stage and servo-control feed unit. The motion parts of X, Y, and Z axes were driven by DC servo motors with the resolution of 0.1 μm. Direct current controlled by a constant voltage is provided from the power supply (IT6322, ITECH Electronics, China) with 1 mA minimum output current and 30 V maximum output voltage. The appearance of the finished surface was examined with 3D profilometer (MicroXAM, ADE, USA) and scanning electron microscope (JSM-5610LV, JEOL, Japan). The dimensions of the structures (length, width, and depth) were measured in the cross-sectional profile which was obtained by 3D profilometer (MicroXAM, ADE, USA).

4 In situ fabrication of cylindrical electrode

The micron scale cylindrical electrode is electrochemically fabricated in this paper. Figure 5 illustrates the unit of cylindrical electrode in situ fabrication which is a part of the experimental system. A tungsten rod as an initial electrode linked to the anode of power supply was located in the center of a stainless barrel. The stainless barrel was not only a container of the electrolyte but also a cathode for electrode etching. The electrode was immerged in 2 M KOH solution at the room temperature of 26°C. When the machining voltage was applied, electrochemical reactions occurred at the electrodes:

The tungsten rod dissolves at the anode by the following electrochemical reactions:

$$\mathrm{W} + 8\mathrm{OH}^- \rightarrow \mathrm{WO_4}^{2-} + 4\mathrm{H_2O} + 6e^-$$

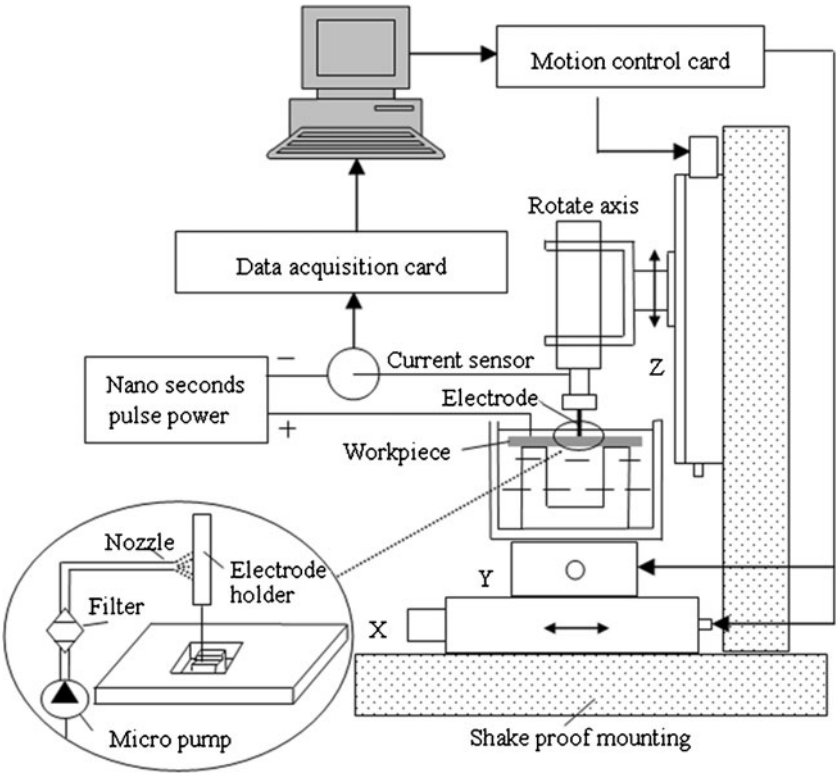

Fig. 4 Sketch of the experimental system

The electrochemical reaction on the cathode is:

$$6H_2O + 6e^- \rightarrow 3H_2 + 6OH^-$$

During the anode process, the tungsten rod was gradually dissolved, and its diameter decreased. Because the tungsten rod was positioned at the center of the barrel, the shape of the rod retained homogeneous cylinder in the whole process of etching. The key problem for in situ fabricating micron scale cylindrical electrode is how to precisely control the diameter of the electrode. It is difficult to on-line monitor the diameter of the electrode, so the diameter is indirectly evaluated by the machining time in the etching process.

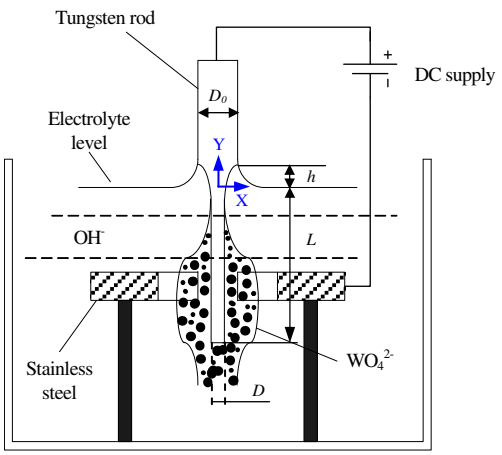

Fig. 5 Sketch of the cylindrical electrode fabricated in situ

In this etching process, according to Faraday laws, the material removal volume V is:

$$V = \frac{A}{\rho z F} Q \tag{13}$$

where A is the atomic molecular weight, ρ is the density, z is the valance of ions, F is the Faraday constant, and Q is the electric charge.

The material removal volume is proportional to the quantity of electric charge, and a formula to describe the relationship between the diameter of the electrode D and the electric charge Q can be given as follows [7–9]:

$$Q = \frac{\pi \rho z F}{4A}\left[\left(L + \frac{4}{5}h\right){D_0}^2 - \left(\frac{8}{15}h + L\right)D^2 - \frac{4}{15}hD_0D\right] \tag{14}$$

where L is the immerging depth, h is the surface tension height which can be considered as a constant and approximately equal to 0.04 mm, D_0 is the initial diameter of the electrode, and D is the real-time diameter of the electrode.

It is found experimentally that the experimental current I_t is linearly decreased according to time. So, the electric charge Q also can be expressed by:

$$Q = \int_0^t (kt + b)dt \tag{15}$$

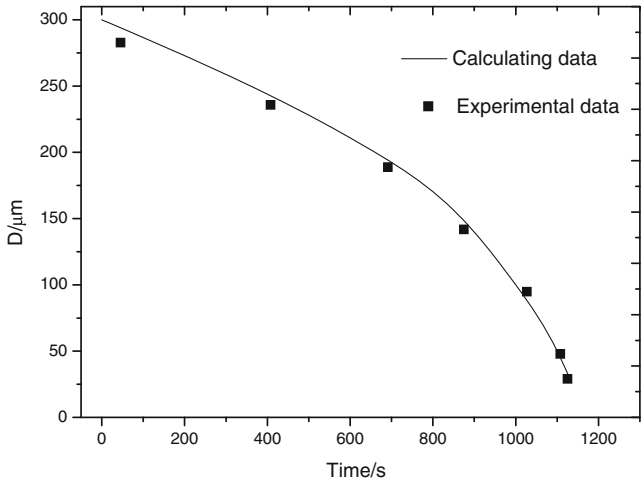

Fig. 6 The change of diameter of the electrode according to machining time

So, the relationship between the real-time diameter of the electrode D and the etching time t can be given as follows:

$$\frac{k}{2}t^2 + bt + C = \frac{\pi\rho zF}{4A}\left[\left(L + \frac{4}{5}h\right)D_0^2 - \left(\frac{8}{15}h + L\right))D^2 - \frac{4}{15}hD_0D\right] \tag{16}$$

where k and b are constants, which are determined by the experimental conditions.

When $t=0$ and $D=D_0$, then the constant $C=0$. So, the time t can be expressed as follows:

$$t = \sqrt{\left(\frac{b}{k}\right)^2 + \frac{\pi\rho zF\left[\left(L+\frac{4}{5}h\right)D_0^2 - \left(\frac{8}{15}h + L\right)D^2 - \frac{4}{15}hD_0D\right]}{2Ak}} - \frac{b}{k} \tag{17}$$

The calculating data based on the proposed model of real-time monitoring of the diameter of the electrode and the experimental data are given in Fig. 6, and the calculating data fit well to the experimental data. As shown in Fig. 6, the diameter of micro cylindrical electrode decreases with the time increment. In the experiment, when the value of the diameter calculated by Eq. (17) was equal to the required diameter of the electrode, the power supply was automatically cut off by using a switch-off control electronic circuit.

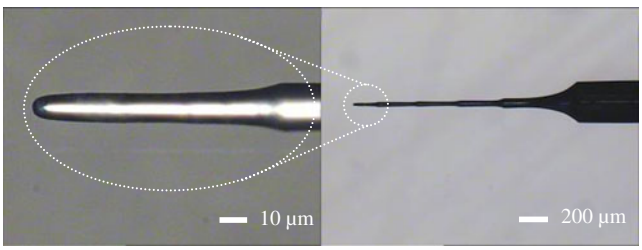

Fig. 7 The cylindrical micro electrode

Table 1 Machining conditions for EMM experiments

Applied voltage (V)	3.5–5.5
Pulse on time (ns)	60–150
Pulse period (μs)	1
Electrode diameter (μm)	3–18
Workpiece material	Super alloy (GH3030)
Electrolyte	0.2 M H_2SO_4 solution
Mill layer thickness (μm)	≤Electrode diameter
Feed rate (μm/s)	0.2–1

Figure 7 shows in situ fabricated micro cylindrical electrode with the diameter of 10 μm. It took about 20 min to produce this cylindrical electrode from a tungsten rod with the initial diameter of 300 μm.

5 Experiments

Experiments of the micro electrochemical milling of a nickel-base superalloy (GH3030) plate with the thickness of 300 μm were carried out to demonstrate the effects of machining parameters on the side gap. As mentioned above, the side gap $^{\Delta}S$ is considered as the evaluation of machining localization [10]. The side gap is dependent on the electrode diameter, pulse voltage, pulse on time, electrolyte concentration, and so on. Table 1 shows the machining conditions for micro electrochemical milling.

In order to verify the mathematical model of micro electrochemical milling, a set of straight groove machining experiments were carried out to investigate the influence of the milling layer thickness and electrode diameter on machining shape precision. Machining conditions of this set of experiments were as follows: electrode diameter of 10 μm, 0.2 mol/L H_2SO_4 electrolyte, machining voltage of 4.5 V, pulse frequency of 1 MHz, pulse on time of 100 ns, and feed rate of 0.2 μm/s. Figure 8a shows the machining result with the milling layer thickness of 15 μm. By contrast, Fig. 8b shows the machining result with the milling layer thickness of 10 μm.

Figure 8 shows that when the layer thickness is greater than the electrode diameter, the shape precision at the starting point will get worse. So, in order to ensure a good

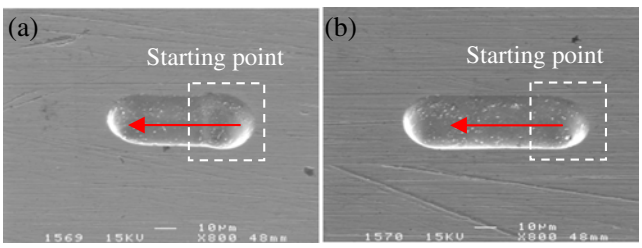

Layer thickness of 15μm Layer thicknessof 10μm

Fig. 8 Effect of layer thickness on shape precision

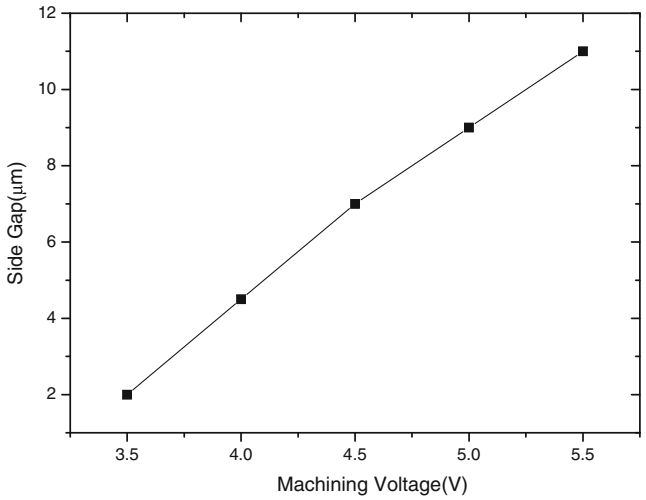

Fig. 9 Variation in side gap with the voltage of pulse (10 μm electrode, 100 ns pulse on time, 1 μs pulse period, 0.2 mol/l H_2SO_4)

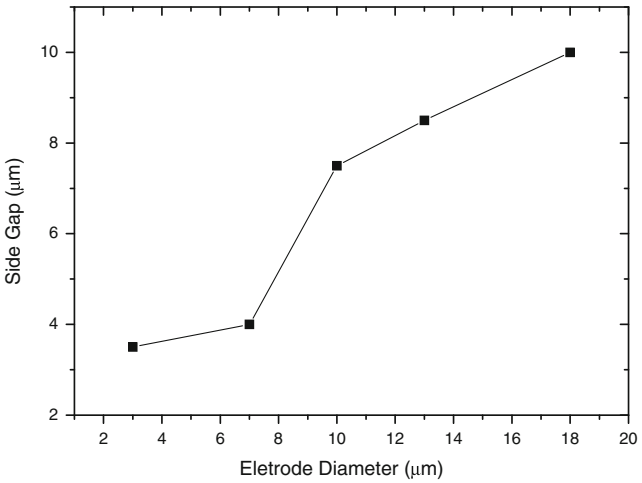

Fig. 11 Variation in side gap with the electrode diameter (4.5 V, 100 ns pulse on time, 1 μs pulse period, 0.2 mol/l H_2SO_4)

shape precision, the milling layer thickness should be smaller or equal to the electrode diameter. This is to say, the experimental results prove that the conclusion of the mathematical model is correct.

Figure 9 shows that the side gap increases with increasing voltage. It proves that the machining localization reduces with the increasing voltage. Due to the increase in voltage, machining current also increases. Faraday's law states that the material removal rate (MRR) is proportional to the machining current. As shown in Fig. 8, the side gap from 3.5 to 5.5 V varies almost linearly. Experimental results reveal that the best machining voltage range is around 4.5 V.

Figure 10 shows that with the increase of pulse on time, the side gap also increases. That is to say, the machining localization becomes poor as the pulse on time increases. Increase in pulse on time implies that more time has been allowed to machine the workpiece for a fixed duration, because only during pulse on time does material removal take place. In other words, with the increase of pulse on time, average current density increases which leads to the increase of dissolution efficiency. So, it is very import to select a relatively smaller pulse on time to improve the machining location under a steady machining process. The suggested range of pulse on time in this paper is between 90 and 100 ns.

Figure 11 shows that with the increase of electrode diameter, the side gap increases rapidly. That is to say, the machining localization will become much better if the electrode diameter is very small. As shown in Fig. 11, the groove width increases slowly at the range of 3–7 μm, and on further increase of electrode diameter in the range of 7–18 μm, the side gap increases rapidly. Therefore, the electrode diameter as small as possible is suggested for the improvement of the machining accuracy.

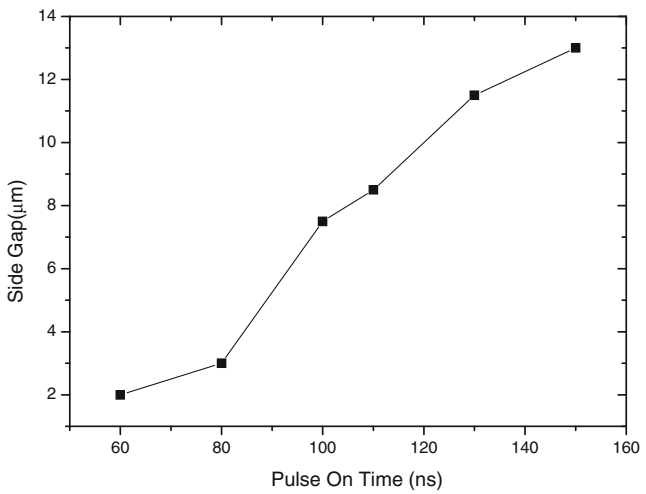

Fig. 10 Variation in side gap with pulse on time (10 μm electrode, 4.5 V, 1 μs pulse period, 0.2 Mol/l H_2SO_4)

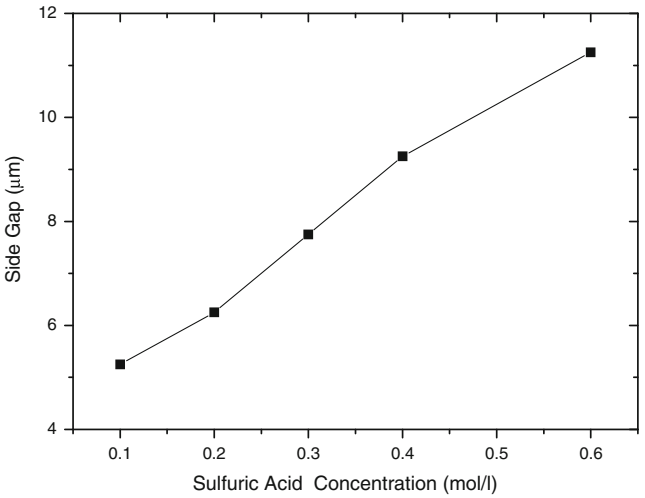

Fig. 12 Variation in side gap with the electrolyte concentration (10 μm electrode, 4.5 V, 100 ns pulse on time, 1 μs pulse period)

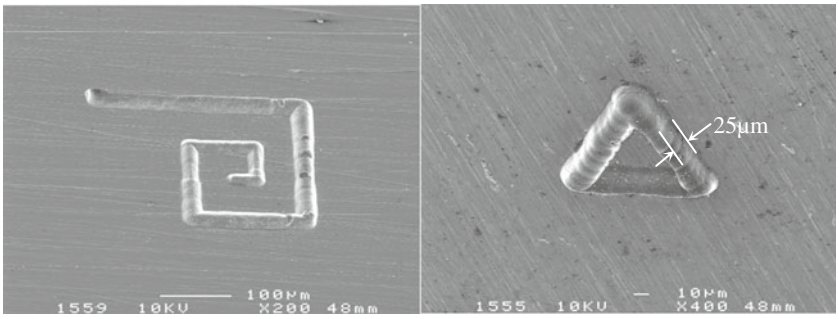

Fig. 13 2D micro complex shapes

Figure 12 shows that, with the electrolyte concentration increases, the side gap increases rapidly and almost linearly. Because of the increase of solution concentration, the solution conductivity increased sharply, which leads to a larger current density during the machining process. So, the MRR of anode increases per unit time, and the machining stability declines rapidly. Therefore, the lower electrolyte concentration is suggested for the improvement of the machining localization. The suggested electrolyte concentration in this paper is about 0.2 M.

Some 2D micro shapes with the width of about 25 μm were machined, as shown in Fig. 13. The micro electrode with the diameter of 10 μm obtained in the electrochemical etching was used as a cathode tool for the micro electrochemical milling.

A 3D structure with three steps was machined as shown in Fig. 14a. The total depth of the cavity was about 45 μm, and each single-step size was about 15×55×15 μm. The milling layer thickness was 5 μm, machining feed rate was 1 μm/s, the nanosecond pulses with pulse amplitude of 4.5 V, pulse on time of 95 ns, and pulse period of 1 μs were used in the machining process. After measurement and calculation, the finished surface roughness Ra of A–A cross section as shown in Fig. 14b is about 0.2 μm. It is proved

Fig. 14 3D micro structure with three steps

(a)

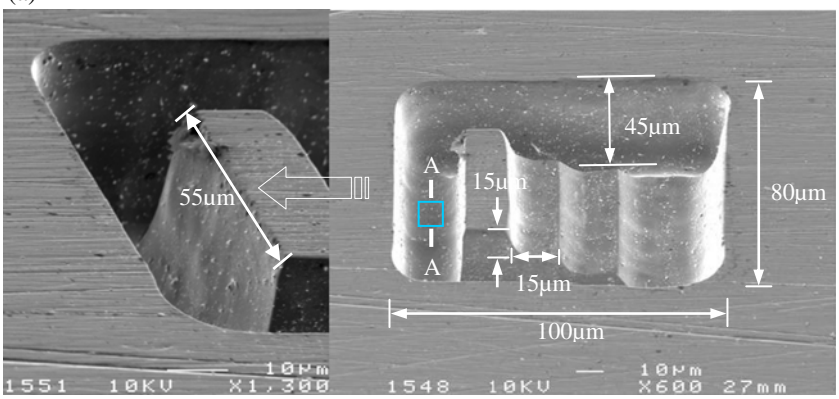

SEM dimension figure

(b)

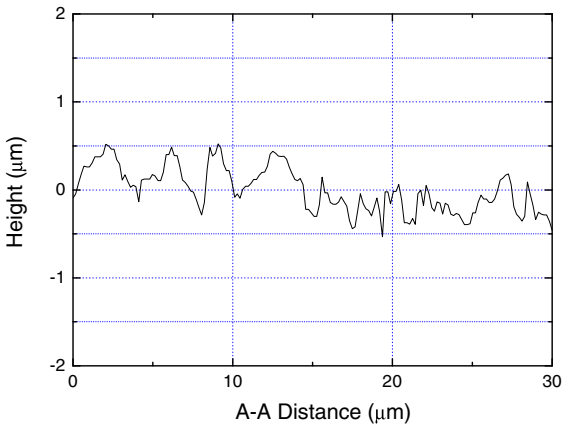

The cross-sectional shape of the finished surface

that the electrochemical micro milling can achieve good shape precision and good surface quality by controlling the machining parameters.

6 Conclusions

In this paper, the micro electrochemical milling by layer process is studied deeply. The mathematical model and the experimental equipment for micro electrochemical milling by layer have been established successfully. After the preliminary experiments, some complex 2D shapes and 3D micro structure were fabricated. The conclusions can be summarized as follows:

1. In order to get a good shape precision, the mathematical model of micro electrochemical milling by layer is established.
2. An EMM system for achieving micron-sized complex structures is developed.
3. The mathematical model for in situ fabricating of the micro cylindrical electrode is built to control the electrode diameter D by controlling the etching time t.
4. In order to get good machining quality, many suggested values of the key machining parameters are proposed.
5. Successful fabrication of the complex micro structure proves that micro electrochemical milling is a promising micromachining technique which can be used to fabricate the complex MEMS parts. For further research, a more complex structure with free surfaces will be fabricated by the micro electrochemical milling technology.

Acknowledgments This work was financially supported by the Chinese National Natural Science Funds (50635040) and the National High-Tech Research and Development Program (863 Program) (2009AA04Z302).

References

1. McGeough JA, Leu MC, Rajurkar KP, De Silva AKM, Liu Q (2001) Electroforming process and application to micro/macro manufacturing. Ann CIRP 50(2):499–514
2. Schuster R, Kirchner V, Allongue P, Ertl G (2000) Electrochemical micromachining. Science 289:98–101
3. Kim BH, Na CW, Lee YS, Choi DK, Chu CN (2005) Micro electrochemical machining of 3D micro structure using dilute sulfuric acid. Ann CIRP 54(1):191–194
4. Trimmer AL, Hudson JL, Kock M, Schuster R (2003) Single-step electrochemical machining of complex nanostructures with ultrashort voltage pulses. Appl Phys Lett 82:3327–3329
5. Lee ES, Baek SY, Cho CR (2005) A study of the characteristics for electrochemical micromachining with ultrashort voltage pulses. Int J Adv Manuf Technol 31:762–769
6. Kim BH, Ryu SH, Choi DK, Chu CN (2005) Micro electrochemical milling. J Micromech Microeng 15(1):124–129
7. Lim YM, Kim SH (2001) An electrochemical fabrication method for extremely thin cylindrical micropin. Int J Mach Tools Manuf 41(15):2287–2296
8. Lim YM, Lim HJ, Liu JR, Kim SH (2003) Fabrication of cylindrical micropins with various diameters using DC current density control. J Mater Process Technol 141:251–255
9. Liu Y, Zhu D, Zeng YB, Yu HB (2011) Development of micro electrodes for electrochemical micromachining. Int J Adv Manuf Technol 55:195–203
10. Li Y, Zheng YF, Yang G, Peng LQ (2003) Localized electrochemical micromachining with gap control. Sensors Actuator A 108:144–148